

# 1 Comparison of advanced echocardiographic right ventricular functional 2 parameters with cardiovascular magnetic resonance in 3 adult congenital heart disease 4

5 Daniel J. Bowen BSc<sup>1</sup>; Robert M. Kauling MD<sup>1</sup>; Chiara Pelosi MD<sup>1</sup>; Lourus van Haveren<sup>1</sup>;  
6 Jackie S. McGhie PhD<sup>1</sup>; Judith A.A.E Cuypers MD, PhD<sup>1</sup>; Alexander Hirsch<sup>1,2</sup>; Jolien W.  
7 Roos-Hesselink MD, PhD<sup>1</sup>; Annemien E. van den Bosch MD, PhD<sup>1</sup>.

8  
9 *<sup>1</sup>Department of Cardiology, Erasmus MC University Medical Center Rotterdam, The  
10 Netherlands*

11 *<sup>2</sup>Department of Radiology and Nuclear Medicine, Erasmus MC University Medical  
12 Center Rotterdam, The Netherlands*

13  
14 Corresponding author:

15 Daniel J. Bowen BSc, Erasmus University Medical Centre, Department of Cardiology, P.O.  
16 box 2040, 3000 CA, Rotterdam, the Netherlands. E-mail: d.bowen@erasmusmc.nl

## 17 Abstract

18 **Aims.** Advanced transthoracic echocardiography (TTE) using volumetric and deformational  
19 indices provides detailed quantification of right ventricular (RV) function in adults with  
20 congenital heart disease (ACHD). Two-dimensional multi-plane echocardiography (2D-MPE)  
21 has demonstrated regional wall differences in RV longitudinal strain (LS). This study aims to  
22 evaluate the association of these parameters with cardiovascular magnetic resonance (CMR).

23 **Methods and results.** One hundred stable ACHD patients with primarily affected RVs were  
24 included (age 50±5 years; 53% male). Conventional and advanced echocardiographic RV  
25 functional parameters were compared to CMR-derived RV function.

26 Advanced echocardiographic RV functional parameters were measurable in approximately one-  
27 half of the study co-hort, whilst multi-wall LS assessment feasibility was lower. CMR RV  
28 ejection fraction (CMR-RVEF) was moderately correlated with deformational, area and  
29 volumetric parameters (RV global LS [lateral wall and septum], n=55: r=-0.62, p<0.001; RV

30 wall average LS, n=34: r=-0.49, p=0.002; RV lateral wall LS, n=56: r=-0.45, p<0.001; fractional  
© The Author(s) 2023. Published by Oxford University Press on behalf of the European Society of Cardiology. This  
is an Open Access article distributed under the terms of the Creative Commons Attribution License  
(<https://creativecommons.org/licenses/by/4.0/>), which permits unrestricted reuse, distribution, and reproduction  
in any medium, provided the original work is properly cited.

1 area change [FAC], n=67: r=0.48, p<0.001; 3D-RVEF, n=48: r=0.40, p=0.005). Conventional  
2 measurements such as TAPSE and RV S' correlated poorly. RV global LS best identified CMR-  
3 RVEF <45% (AUC: 0.84, p<0.001: cut-off value -19%: sensitivity 100%, specificity 57%).  
4 RVEF and LS values were significantly higher when measured by CMR compared to TTE (mean  
5 difference RVEF: 5[-9 to 18]%; lateral (free) wall LS: -7[7 to -21]%; RV global LS: -6 [5 to -  
6 16]%) whilst there was no association between respective LS values.

7 **Conclusion.** In ACHD patients, advanced echocardiographic RV functional parameters are  
8 moderately correlated with CMR-RVEF, although significant differences exist between indices  
9 measurable by both modalities.

10 **Keywords:** 3D echocardiography; multi-plane echocardiography; cardiovascular magnetic  
11 resonance; right ventricular longitudinal strain; speckle tracking; feature tracking.

## 12 **Introduction**

13 Evaluation of right ventricular (RV) function by trans-thoracic echocardiography (TTE) can  
14 often be challenging in adults with congenital heart disease (ACHD), particularly in instances of  
15 altered cardiovascular and musculoskeletal anatomy or following multiple surgical interventions  
16 (1). Whilst conventional indices which evaluate RV longitudinal shortening are highly feasible  
17 and reproducible, the addition of advanced deformational or volumetric parameters is preferable  
18 to enhance RV functional assessment (2). As the global population of ACHD patients continues  
19 to grow and age, the dependency on cardiovascular magnetic resonance (CMR) to provide  
20 accurate assessment of RV function will increase. However, as a more accessible modality,  
21 echocardiography has an important role to play in reducing the burden on CMR (3). For ACHD  
22 patients with good to reasonable echocardiographic image quality, it is important to define which

1 functional measurements demonstrate an acceptable level of agreement with CMR. Several  
2 studies have investigated the association between conventional and advanced echocardiographic  
3 parameters and CMR in ACHD populations (1, 4-7). In this study, we also include two-  
4 dimensional multi-plane echocardiographic (2D-MPE) imaging, which enables quantitative  
5 assessment of four different RV free wall regions from one apical acoustic window using  
6 electronic plane rotation (8). We previously reported high feasibility for quantification of RV  
7 function with 2D-MPE in ACHD populations and provided new insights into regional RV wall  
8 deformation (9, 10). The performance of regional RV wall deformation compared to CMR has  
9 however not yet been demonstrated. Furthermore, with the emergence of CMR feature tracking  
10 (CMR-FT) (11), it is of interest to investigate how comparable longitudinal strain (LS)  
11 measurements are with speckle tracking echocardiography (STE) in this patient population. This  
12 study therefore aims to evaluate the association of these parameters, alongside other  
13 conventional and advanced echocardiographic indices with reference CMR-derived RV function  
14 in ACHD.

## 15 **Methods**

### 16 *Study population*

17 The study population consists of ACHD patients who participated in the Quality of Life 4 study  
18 at the Erasmus Medical Center (EMC) in Rotterdam, between February 2020 and September  
19 2021. The Quality of Life study was initiated by EMC in 1990 and is performed every 10 years.  
20 The study follows up individuals born with ACHD whose primary surgical repair took place  
21 before the age of fifteen years old between 1968-1980. For this study, only individuals with  
22 initial pathologies primarily affecting the RV were included, diagnoses were atrium septum

1 defect (ASD), Tetralogy of Fallot (ToF) and pulmonary stenosis (PS). Subjects were excluded  
2 from analysis if CMR and TTE were not performed on the same day. The study was carried out  
3 according to the principles of the Declaration of Helsinki, was approved by the local medical  
4 ethics committee (MEC-2019 0465), and written informed consent was obtained from all  
5 subjects.

#### 6 *Echocardiographic acquisition and conventional measurements*

7 An extensive TTE protocol was carried out according to international guidelines (12) with  
8 additional focus on RV structure and function by acquiring 2D-MPE and 3D-TTE recordings in  
9 individuals where image quality permitted. All echocardiograms were performed by one of two  
10 echocardiographers (DB, LH) specialised in congenital echocardiography. Studies were acquired  
11 using an EPIQ7 ultrasound system (Philips Medical Systems, Best, The Netherlands) equipped  
12 with an X5-1 matrix array transducer (composed of 3040 elements with 1-5MHz). Single beat  
13 3D recordings of the right heart were acquired using Heart Model software (Philips Medical  
14 Systems). Conventional 2D echocardiographic parameters for left and right heart size and  
15 function were collected in addition to the grading of any valvular lesions as either less than (<) or  
16 equal or greater than ( $\geq$ ) moderate in severity using parameters as documented in published  
17 guidelines (13, 14). RV basal, mid and longitudinal linear dimensions alongside fractional area  
18 change (FAC, calculated as end-diastolic area–end-systolic area/end-diastolic area x 100) were  
19 measured in the standard focused RV apical four chamber view. Tricuspid annular plane systolic  
20 excursion (TAPSE) and tissue Doppler imaging derived tricuspid annular peak systolic velocity  
21 (RV-S') were measured at the basal lateral RV wall.

#### 22 *Advanced right ventricular assessment by 2D multi-plane and 3D echocardiography*

1 The evaluation of regional RV wall function by 2D multi-plane echocardiography has been well  
2 documented in our previous publications (8, 9). In short, from a fixed apical probe position,  
3 electronic plane rotation around the RV apex allows visualisation of different RV free wall  
4 regions. Each RV wall is confirmed by the presence of a certain left-sided landmark associated  
5 with an approximate degree of electronic rotation. The first view at  $0^\circ$  shows the lateral RV wall  
6 with the left sided landmark being the mitral valve. The second view at approximately  $+40^\circ$   
7 shows the anterior RV wall and the coronary sinus, thirdly at approximately  $-40^\circ$  the inferior RV  
8 wall and the aortic valve and lastly at approximately  $-90^\circ$  the inferior coronal view with the  
9 inferior wall and the anterior segment of the RV outflow tract (RVOT) (figure 1). The four RV  
10 wall datasets were digitally exported to a vendor-neutral server (TomTec Imaging Systems,  
11 Unterschleissheim, Germany) and data analysis was performed offline by one independent  
12 observer (DB) using DICOM greyscale images. To assess peak systolic RV LS, an RV algorithm  
13 wall motion tracking software was used (2D CPA, Image-Arena version 4.6; TomTec Imaging  
14 Systems). The endocardial border of the RV free wall and septum were manually traced at end-  
15 systole and adjusted accordingly in end-diastole if required. This was performed in each of the  
16 four multi-plane views previously described. A single segment peak LS value for each RV wall  
17 was derived from the average of the basal, mid and apical segments. Global LS was calculated by  
18 averaging the strain values of the lateral wall and inter-ventricular septum. An RV wall average  
19 value was calculated when LS of the lateral, anterior and inferior walls were all feasible to  
20 measure in an individual. The 3D datasets were digitally exported to the same TomTec server  
21 and analysed retrospectively by DB using specialised RV analysis software (TomTec 4D-RV  
22 function 2.0). After placing set landmarks, RV volumes (indexed for body surface area) and

1 ejection fraction (RVEF) were automatically calculated over the entire cardiac cycle. All  
2 contours were checked and manually adjusted when necessary.

### 3 *Cardiovascular magnetic resonance*

4 CMR examinations were performed on a clinical 1.5T MRI system (SIGNA Artist, GE  
5 Healthcare, Milwaukee, WI, USA) with a dedicated cardiac or anterior array coil,  
6 electrocardiographic gating, and breath-hold techniques. Standard balanced steady-state free  
7 precession (bSSFP) cine images were obtained during end-expiratory breath-hold in standard  
8 three long-axis views (2-, 3-, and 4- chamber) and in a contiguous stack of short-axis (SA)  
9 views, with coverage from base to apex. bSSFP scan parameters were: slice thickness long-axis  
10 8mm and SA 6mm, interslice gap 4mm, TR/TE 3.8/1.7 ms, flip angle 65°, ASSET 2, acquired  
11 matrix long-axis 280x200 and SA 200x200, and 30 phases per cardiac cycle. CMR analysis was  
12 performed on anonymized images by an experienced CMR reader (JAC). Functional analysis  
13 was performed on SA images using automatic segmentation of the epi- and endocardial contours  
14 in end-systolic and end-diastolic phase, with inclusion of papillary muscles and trabeculations in  
15 the left ventricular and RV volume. All contours were checked and manually adjusted when  
16 necessary. Endocardial RV LS was measured in the 4 chamber long axis using CMR-FT. The  
17 RV endocardial contours were drawn manually during the end-diastolic and end-systolic phase  
18 by one operator (DB). Subsequently, the software automatically traced the cardiac contours  
19 during the cardiac cycle, resulting in the calculation of peak LS of the RV free wall and inter-  
20 ventricular septum. Global LS was calculated as the average of these two values as per TTE.  
21 CMR analyses were performed using commercially available software (Qmass version 8.1 and  
22 QStrain version 4.0, Medis Medical Imaging Systems, Leiden, The Netherlands). All analyses  
23 were performed blinded to the results of the other imaging modality.

## 1 *Statistical analysis*

2 The distribution of data was assessed using histograms and the Shapiro–Wilk test. Continuous  
3 data is presented as mean  $\pm$  standard deviation (SD) or median [inter-quartile range], whilst  
4 categorical data is presented as frequencies. The paired T-test or Wilcoxon signed rank test was  
5 used for comparison of within-subject LS values and for RV functional parameters measurable  
6 by both TTE and CMR. Linear regression analysis was performed to evaluate the association  
7 between echocardiographic RV functional parameters and CMR-derived RVEF, in addition to  
8 LS values measured by both modalities (RV lateral [free] wall and RV global LS). Pearson’s  
9 correlation coefficient ( $r$ ) is reported and interpreted as follows:  $<0.2$  = poor,  $0.20$ - $0.39$  = fair,  
10  $0.40$ - $0.59$  = moderate,  $0.60$ - $0.79$  = good, and  $0.80$ - $1.00$  = excellent. Receiver operating  
11 characteristic (ROC) curves were created to determine the ability of echocardiographic  
12 parameters to detect reduced CMR-RVEF (cut-off value of 45% used (15)). The area under the  
13 curve (AUC) is reported in addition to the ‘optimal’ cut off value for each parameter to detect  
14 reduced RVEF. This is defined as the value which corresponds with the highest Youden-J index  
15 (specificity + sensitivity – 1), whereby a value of 1 indicates perfect detection and a value of 0  
16 no detection. Agreement between CMR-derived and TTE-derived measurements was evaluated  
17 using Bland-Altman analysis (16). The agreement between two measurements was determined as  
18 the mean of the differences  $+1.96$  times their SD. Additionally, the coefficient of variation was  
19 provided (SD of the differences of two measurements divided by their mean value, times 100).  
20 All statistical analyses were performed using the Statistical Package for Social Sciences version  
21 25 (SPSS, Inc., Armonk, NY, USA). The statistical tests were two-sided and a p-value  $<0.05$  was  
22 considered statistically significant.

## 23 **Results**

1 One-hundred ACHD patients (age  $50 \pm 5$  years, 53% male) were included (figure 2), all with  
2 initial pathologies primarily affecting the RV (ASD  $n = 48$ ; ToF  $n = 32$ ; PS  $n = 20$ ). Age at  
3 definitive surgical correction was 6 [3, 8] years, whilst 25 individuals had undergone surgical re-  
4 intervention. Demographics, electrocardiogram and echocardiographic characteristics are  
5 detailed in table 1. Very few patients had  $\geq$  moderate right sided valve disease: pulmonary valve  
6 insufficiency – in 11 patients; pulmonary valve stenosis – in 8; tricuspid regurgitation – in 5.  
7 Only 1 individual had significantly reduced left ventricular systolic function and 5 individuals  
8 had high grade (II/III) diastolic dysfunction.

### 9 *Measurement feasibility*

10 Measurements of all echocardiographic functional indices were attempted in all patients where  
11 image quality permitted. The measurement feasibility of each parameter is demonstrated in  
12 figure 3. Conventional parameters were the most feasible to perform (TAPSE in 98 patients; RV  
13 S' in 93; FAC in 67). RV lateral wall and global LS were the most feasible deformational  
14 parameters (in 57 and 55, respectively) and more performable than 3D-RVEF (in 48). LS  
15 measurement feasibility was lower in the other RV walls with three walls measurable in 34  
16 individuals. CMR volumetric measurements were performed in all patients. LS measurements  
17 using CMR-FT were performed in 98 patients of which 56 RV lateral (free) wall and 55 RV  
18 global LS values were comparable with those of STE. All echocardiographic parameters are  
19 demonstrated in table 2, with those of CMR in table 3. RV global LS was significantly lower  
20 than RV lateral wall LS ( $-19 \pm 4\%$  vs  $-22 \pm 5\%$ ,  $p < 0.001$ ). Differences across the RV walls were  
21 evident, although only inferior coronal view wall LS was significantly lower than lateral wall LS  
22 ( $-19 \pm 4\%$ ,  $p = 0.004$ ).



## 1 *Comparison with CMR*

2 The associations between CMR-RVEF and the best performing echocardiographic functional  
3 parameters were moderate (table 2). 3D-TTE-derived RV volumes and RVEF were significantly  
4 lower than those derived by CMR (RVEDVi: 74 [61, 88] ml/m<sup>2</sup> vs 100 [86, 119] ml/m<sup>2</sup>, p  
5 <0.001; RVESVi: 38 [33, 50] ml/m<sup>2</sup> vs 49 [40, 60] ml, p <0.001; RVEF 46 ± 6% vs 51 ± 6%, p  
6 <0.001). The association between 3D-RVEF and CMR-RVEF was moderate (r = 0.40, p =  
7 0.005) with a mean difference of 5 [-9 to 18] % between respective measurements (co-efficient  
8 of variation [CoV] -14%, figure 4). Of the deformational parameters, global LS (r = -0.62, p  
9 <0.001), lateral wall LS (r = -0.45, p <0.001), anterior wall LS (r = -0.41, p = 0.007) and RV  
10 wall average LS (r = -0.49, p = 0.002) values correlated strongest with CMR-RVEF. Of the  
11 conventional parameters, FAC correlated strongest with CMR-RVEF (r = 0.48, p <0.001)  
12 however there was no association with TAPSE (r = 0.16, p = 0.06) or RV S' (r = 0.23, p = 0.23).  
13 RV LS values were significantly higher when measured by CMR-FT than by STE (lateral [free]  
14 wall LS: -29 ± 5% vs -22 ± 5%, p <0.001; global LS -24% ± 4% vs -18 ± 5, p <0.001). There  
15 was a mean difference of -7 [7 to -21] % between lateral (free) wall LS measurements (CoV -  
16 28%) and -6 [5 to -16] % between global LS measurements (CoV - 25%). Furthermore, there  
17 was no association between respective strain values (lateral [free] wall LS: r = 0.12, p = 0.37;  
18 global LS: r = 0.09, p = 0.49).

19 RV dysfunction was identified in 23 patients using the criteria of a CMR-RVEF <45%. Receiver  
20 operating characteristic (ROC) curve analysis (table 4, figure 5) revealed RV global LS to be the  
21 best identifier of CMR-RVEF <45% (AUC: 0.84 [0.72-0.96], p <0.001: cut-off value of -19%:  
22 sensitivity 100%, specificity 57%), with statistical significance compared to RV lateral wall LS  
23 (AUC: 0.76 [0.60-0.92], p = 0.04), TAPSE (AUC: 0.60 [0.46-0.74], p = 0.03) and FAC (AUC:

1 0.68 [0.52-0.83],  $p = 0.01$ ). In the context of a low number of observations, differences between  
2 the AUC of other parameters were not statistically significant ( $p > 0.05$ ).

### 3 **Discussion**

4 Accurate assessment of RV function is essential when following up ACHD patients, with  
5 echocardiography the first line imaging modality available to the cardiologist. In recent years,  
6 advances in ultrasound probe technology and quantification software have opened up new  
7 possibilities for the evaluation of RV function. In this study of ACHD patients, advanced  
8 echocardiographic RV functional indices such as 3D-RVEF and RV LS were moderately  
9 correlated with reference CMR-derived RVEF. However, significant differences were observed  
10 between indices measurable by both modalities. Conventional FAC provided a comparable  
11 representation of CMR-RVEF to that of 3D-RVEF and RV LS and was more feasible to perform.  
12 Whilst highly feasible, TAPSE and S' measurements correlate poorly with CMR-RVEF and  
13 should not be used in isolation to evaluate RV function in ACHD patients. LS averaged across  
14 multiple RV walls did not associate significantly better with CMR-RVEF than the global or  
15 lateral (free) wall values. 2D-MPE may only provide additional functional information when  
16 notable regional wall motion abnormalities are present, such as in ToF (figure 6).

#### 17 *Conventional echocardiographic parameters*

18 Conventional TTE parameters which assess longitudinal function at the basal RV inlet (TAPSE,  
19 RV S') correlated poorly with CMR-RVEF. In ACHD patients, these measurements do not  
20 represent global RV function if regional abnormalities are present (17). Furthermore, basal RV  
21 longitudinal contraction in post-operative ACHD populations is known to be affected by  
22 pericardiectomy, even long term post-surgery (18).

1 Meanwhile, FAC correlated moderately with CMR-RVEF and was comparable to 3D-RVEF and  
2 RV LS. FAC is however geometry and load dependent and does not include the contribution of  
3 the RVOT to RV ejection (19). In ToF patients with dysfunctional RVOT for instance, FAC will  
4 often result in an overestimation of global RV function (2). Still, this is a useful conventional  
5 parameter to use in an ACHD population and in this study, FAC did not perform inferiorly to  
6 3D-RVEF.

### 7 *Advanced echocardiographic parameters*

8 Most RV wall LS values correlated moderately with CMR-RVEF, however multiple wall  
9 average values were not superior to LS measurements from the standard apical four chamber  
10 view. Whilst 2D-MPE enables a more global RV deformational analysis to be performed, this  
11 appears more pertinent to ACHD with abnormalities of the RVOT, such as ToF. Here, anterior  
12 wall deformation is reduced (9), with proximity to a dyskinetic RVOT a likely factor following  
13 initial repair or subsequent re-intervention (2). CMR studies have also demonstrated the presence  
14 of fibrosis in adult patients in the surrounding myocardial segments (20, 21).

15 3D-RVEF correlated less strongly with CMR-RVEF than LS or FAC measurements and  
16 underestimated RV volumes and ejection fraction. This has been widely identified in previous  
17 3D TTE-CMR comparative studies, which report that whilst volumes generally correlate well,  
18 those of 3D-TTE are 20-34% smaller (1, 4, 7). Some studies have however reported better  
19 association between respective RVEF measurements (6, 7). A major limitation of 3D TTE is the  
20 poor visualisation of the anterior RV wall. Artefact from the sternum, scar tissue or intra-cardiac  
21 prosthetic material related to previous surgical interventions leads to echo drop out and volume  
22 underestimation (4). In contrast, CMR is less limited by near field resolution and thus  
23 endocardial borders can be better delineated (2). Furthermore, in significantly dilated and/or

1 abnormally shaped RVs, 3D-TTE may fail to fully accommodate the entire chamber within the  
2 pyramidal dataset. This can also lead to foreshortening of the RV apex and significant  
3 underestimation of RV volumes (2, 4).

4 RV lateral (free) wall and global LS values were significantly greater (i.e. more negative) when  
5 measured by CMR-FT than by STE. The poor agreement between values may be due to  
6 differences in image processing software and the inability to achieve the same imaging plane.  
7 RV LS derived by CMR-FT is however not by definition less useful than STE and has been  
8 shown to be an independent predictor of adverse events and mortality (22, 23). Differences in  
9 image resolution between TTE and CMR should also be considered. Spatial resolution is higher  
10 in CMR images, enabling more accurate tracking of the RV endocardium than by TTE. On the  
11 other hand, temporal resolution in the CMR loops was much lower (30 frames per cardiac cycle)  
12 than that recorded for TTE strain analysis (>60 frames per second). Lower temporal resolution  
13 results in larger distances covered by the features between frames and requires an enlarged  
14 interrogation window, which may decrease accuracy (24). Nonetheless, it has been reported that  
15 acquisitions at 30 frames per cardiac cycle offer consistent strain assessments in CMR when  
16 compared to higher temporal resolutions (25). A lower signal to noise ratio in TTE means that  
17 some segments of the myocardium may not be adequately imaged throughout the cardiac cycle  
18 and require averaging of the measured values to fill these gaps (24). Lastly, CMR strain analysis  
19 was performed on a different vendor to that of TTE, and significant inter-vendor variability has  
20 been previously described for CMR-derived RV LS measurements (26).

### 21 *Clinical impact and future directions*

22 Our findings demonstrate that where feasible, advanced echocardiographic RV functional  
23 parameters can be incorporated into routine ACHD follow up, albeit with the awareness of the

1 differences that exist with CMR-derived measurements. The increasing availability of automated  
2 RV 3D and strain software modalities on the echo machine will help to facilitate the transition to  
3 daily clinical practice (27, 28). Technological advances may make 3D-STE of the RV feasible  
4 and attractive in the coming years. In a recent publication, Mocerì et al. demonstrated strain  
5 analysis of multiple RV regions derived from one 3D acquisition in congenital and healthy  
6 populations (29). Quantification currently requires much post-processing using custom built  
7 programmes and therefore this technique is not yet ready for clinical practice.

### 8 *Limitations*

9 The study population suffers from some selection bias as reduced CMR-RVEF was present in  
10 only 23 patients. Although low levels of RV dysfunction were unforeseen, a greater proportion  
11 of impaired RV's are required to adequately investigate the ability of echocardiographic  
12 parameters to identify reduced CMR-RVEF. Due to lower feasibility of 3D-RVEF and multi-RV  
13 wall LS indices, evaluation by disease group was deemed insufficient to report. Despite  
14 including a relatively large number of ACHD patients undergoing same day TTE and CMR, a  
15 larger sample size would therefore be desirable for future studies.

### 16 **Conclusion**

17 In ACHD patients, advanced echocardiographic RV functional indices are moderately correlated  
18 with reference CMR-derived RV function, although significant differences exist between indices  
19 measurable by both modalities. 3D-RVEF, LS and/or FAC should be used to quantify RV  
20 function when image quality is adequate. Multi-RV wall evaluation may only provide additional  
21 functional information when notable regional wall motion abnormalities are present.

## 1 **Data availability**

2 The data underlying this article will be shared on reasonable request to the corresponding author.

## 3 **Disclosures**

4 Conflicts of Interest: None declared

## 5 **References**

- 6 1. Crean AM, Maredia N, Ballard G, Menezes R, Wharton G, Forster J, et al. 3D Echo  
7 systematically underestimates right ventricular volumes compared to cardiovascular magnetic  
8 resonance in adult congenital heart disease patients with moderate or severe RV dilatation. *J*  
9 *Cardiovasc Magn Reson*. 2011;13(1):78.
- 10 2. Mertens LL, Friedberg MK. Imaging the right ventricle--current state of the art. *Nat Rev*  
11 *Cardiol*. 2010;7(10):551-63.
- 12 3. van der Zwaan HB, Helbing WA, McGhie JS, Geleijnse ML, Luijnenburg SE, Roos-  
13 Hesselink JW, et al. Clinical value of real-time three-dimensional echocardiography for right  
14 ventricular quantification in congenital heart disease: validation with cardiac magnetic resonance  
15 imaging. *J Am Soc Echocardiogr*. 2010;23(2):134-40.
- 16 4. Grewal J, Majdalany D, Syed I, Pellikka P, Warnes CA. Three-dimensional  
17 echocardiographic assessment of right ventricular volume and function in adult patients with  
18 congenital heart disease: comparison with magnetic resonance imaging. *J Am Soc Echocardiogr*.  
19 2010;23(2):127-33.

- 1 5. Kavurt AV, Pac FA, Koca S, Mutlu Mihcioglu A, Yigit H. The evaluation of right  
2 ventricular systolic function in patients with repaired Tetralogy of Fallot by conventional  
3 echocardiographic methods and speckle tracking echocardiography: Compared with the gold  
4 standard cardiac magnetic resonance. *Echocardiography*. 2019;36(12):2251-8.
- 5 6. Khoo NS, Young A, Occleshaw C, Cowan B, Zeng IS, Gentles TL. Assessments of right  
6 ventricular volume and function using three-dimensional echocardiography in older children and  
7 adults with congenital heart disease: comparison with cardiac magnetic resonance imaging. *J Am  
8 Soc Echocardiogr*. 2009;22(11):1279-88.
- 9 7. van der Zwaan HB, Geleijnse ML, McGhie JS, Boersma E, Helbing WA, Meijboom FJ,  
10 et al. Right ventricular quantification in clinical practice: two-dimensional vs. three-dimensional  
11 echocardiography compared with cardiac magnetic resonance imaging. *Eur J Echocardiogr*.  
12 2011;12(9):656-64.
- 13 8. McGhie JS, Menting ME, Vletter WB, Frowijn R, Roos-Hesselink JW, van der Zwaan  
14 HB, et al. Quantitative assessment of the entire right ventricle from one acoustic window: an  
15 attractive approach. *Eur Heart J Cardiovasc Imaging*. 2017;18(7):754-62.
- 16 9. Bowen DJ, van Berendoncks AM, McGhie JS, Roos-Hesselink JW, van den Bosch AE.  
17 Multi-plane echocardiographic assessment of right ventricular function in adults with repaired  
18 Tetralogy of Fallot. *The International Journal of Cardiovascular Imaging*. 2021;37(10):2905-15.
- 19 10. Van Berendoncks AML, Bowen DJ, McGhie J, Cuypers J, Kauling RM, Roos-Hesselink  
20 J, et al. Quantitative assessment of the entire right ventricle from one acoustic window: An  
21 attractive approach in patients with congenital heart disease in daily practice. *International  
22 Journal of Cardiology*. 2021;331:75-81.

- 1 11. Schuster A, Hor KN, Kowallick JT, Beerbaum P, Kutty S. Cardiovascular Magnetic  
2 Resonance Myocardial Feature Tracking: Concepts and Clinical Applications. *Circ Cardiovasc*  
3 *Imaging*. 2016;9(4):e004077.
- 4 12. Lang RM, Badano LP, Mor-Avi V, Afilalo J, Armstrong A, Ernande L, et al.  
5 Recommendations for cardiac chamber quantification by echocardiography in adults: an update  
6 from the American Society of Echocardiography and the European Association of  
7 Cardiovascular Imaging. *Eur Heart J Cardiovasc Imaging*. 2015;16(3):233-70.
- 8 13. Lancellotti P, Tribouilloy C, Hagendorff A, Popescu BA, Edvardsen T, Pierard LA, et al.  
9 Recommendations for the echocardiographic assessment of native valvular regurgitation: an  
10 executive summary from the European Association of Cardiovascular Imaging. *Eur Heart J*  
11 *Cardiovasc Imaging*. 2013;14(7):611-44.
- 12 14. Van Berendoncks A, Van Grootel R, McGhie J, van Kranenburg M, Menting M, Cuypers  
13 J, et al. Echocardiographic parameters of severe pulmonary regurgitation after surgical repair of  
14 tetralogy of Fallot. *Congenit Heart Dis*. 2019;14(4):628-37.
- 15 15. Petersen SE, Aung N, Sanghvi MM, Zemrak F, Fung K, Paiva JM, et al. Reference  
16 ranges for cardiac structure and function using cardiovascular magnetic resonance (CMR) in  
17 Caucasians from the UK Biobank population cohort. *J Cardiovasc Magn Reson*. 2017;19(1):18.
- 18 16. Bland JM, Altman DG. Statistical methods for assessing agreement between two methods  
19 of clinical measurement. *Lancet*. 1986;1(8476):307-10.
- 20 17. Morcos P, Vick GW, 3rd, Sahn DJ, Jerosch-Herold M, Shurman A, Sheehan FH.  
21 Correlation of right ventricular ejection fraction and tricuspid annular plane systolic excursion in  
22 tetralogy of Fallot by magnetic resonance imaging. *Int J Cardiovasc Imaging*. 2009;25(3):263-  
23 70.



- 1 18. Bonnemains L, Stos B, Vaugrenard T, Marie PY, Odille F, Boudjemline Y.  
2 Echocardiographic right ventricle longitudinal contraction indices cannot predict ejection  
3 fraction in post-operative Fallot children. *Eur Heart J Cardiovasc Imaging*. 2012;13(3):235-42.
- 4 19. Rudski LG, Lai WW, Afilalo J, Hua L, Handschumacher MD, Chandrasekaran K, et al.  
5 Guidelines for the echocardiographic assessment of the right heart in adults: a report from the  
6 American Society of Echocardiography endorsed by the European Association of  
7 Echocardiography, a registered branch of the European Society of Cardiology, and the Canadian  
8 Society of Echocardiography. *J Am Soc Echocardiogr*. 2010;23(7):685-713; quiz 86-8.
- 9 20. Babu-Narayan SV, Kilner PJ, Li W, Moon JC, Goktekin O, Davlouros PA, et al.  
10 Ventricular fibrosis suggested by cardiovascular magnetic resonance in adults with repaired  
11 tetralogy of fallot and its relationship to adverse markers of clinical outcome. *Circulation*.  
12 2006;113(3):405-13.
- 13 21. Wald RM, Haber I, Wald R, Valente AM, Powell AJ, Geva T. Effects of regional  
14 dysfunction and late gadolinium enhancement on global right ventricular function and exercise  
15 capacity in patients with repaired tetralogy of Fallot. *Circulation*. 2009;119(10):1370-7.
- 16 22. Romano S, Dell'atti D, Judd RM, Kim RJ, Weinsaft JW, Kim J, et al. Prognostic value of  
17 feature-tracking right ventricular longitudinal strain in severe functional tricuspid regurgitation: a  
18 multicenter study. *Cardiovascular Imaging*. 2021;14(8):1561-8.
- 19 23. Sun W, Yuan Y, Shen X, Zhang Y, Dong N, Wang G, et al. Prognostic value of feature-  
20 tracking right ventricular longitudinal strain in heart transplant recipients. *European Radiology*.  
21 2022:1-11.

- 1 24. Pedrizzetti G, Claus P, Kilner PJ, Nagel E. Principles of cardiovascular magnetic  
2 resonance feature tracking and echocardiographic speckle tracking for informed clinical use. *J*  
3 *Cardiovasc Magn Reson*. 2016;18(1):51.
- 4 25. Backhaus SJ, Metschies G, Billing M, Schmidt-Rimpler J, Kowallick JT, Gertz RJ, et al.  
5 Defining the optimal temporal and spatial resolution for cardiovascular magnetic resonance  
6 imaging feature tracking. *J Cardiovasc Magn Reson*. 2021;23(1):60.
- 7 26. Gertz RJ, Lange T, Kowallick JT, Backhaus SJ, Steinmetz M, Staab W, et al. Inter-  
8 vendor reproducibility of left and right ventricular cardiovascular magnetic resonance  
9 myocardial feature-tracking. *PLoS One*. 2018;13(3):e0193746.
- 10 27. N.V. KP. AutoStrain LV/RV/LA – automated strain measurements 2019 [Available  
11 from: [https://www.philips.com/c-dam/b2bhc/master/landing-pages/cvx/epiq-cvx-autostrain-](https://www.philips.com/c-dam/b2bhc/master/landing-pages/cvx/epiq-cvx-autostrain-white-paper-vmq-5-0-fnl.pdf)  
12 [white-paper-vmq-5-0-fnl.pdf](https://www.philips.com/c-dam/b2bhc/master/landing-pages/cvx/epiq-cvx-autostrain-white-paper-vmq-5-0-fnl.pdf).
- 13 28. N.V. KP. 3D Auto RV — right ventricular quantification 2019 [Available from:  
14 [https://www.philips.com/c-dam/b2bhc/master/landing-pages/cvx/epiq-cvx-3d-auto-rv-white-](https://www.philips.com/c-dam/b2bhc/master/landing-pages/cvx/epiq-cvx-3d-auto-rv-white-paper.pdf)  
15 [paper.pdf](https://www.philips.com/c-dam/b2bhc/master/landing-pages/cvx/epiq-cvx-3d-auto-rv-white-paper.pdf).
- 16 29. Mocerri P, Duchateau N, Gillon S, Jaunay L, Baudouy D, Squara F, et al. Three-  
17 dimensional right ventricular shape and strain in congenital heart disease patients with right  
18 ventricular chronic volume loading. *Eur Heart J Cardiovasc Imaging*. 2021;22(10):1174-81.

## 19 **Figure legends**

20 Figure 1. Advanced echocardiographic imaging for the assessment of RV function. Top left  
21 panel (A) – right ventricular longitudinal strain. Top right panel (B) – 3D right ventricular  
22 ejection fraction. Lower panels (from left to right) – 2D multi-plane echocardiography  
23 (approximate degrees of electronic rotation, RV wall visualised): C – RV-focused apical four

1 chamber view (0°, lateral wall); D – coronary sinus view (+40°, anterior wall); E – aortic view (-  
2 40°, inferior wall); F – coronal view (-90°, inferior wall and RVOT). RV – right ventricle; LV -  
3 left ventricle; CS - coronary sinus; AoV - aortic valve; RVOT - right ventricular outflow tract.

4 Figure 2. Study inclusion.

5 Figure 3. Feasibility of echocardiographic right ventricular functional parameters. TAPSE –  
6 tricuspid annular plane systolic excursion; RV S' - tricuspid annular peak systolic velocity; FAC  
7 – fractional area change; LS – longitudinal strain; RV global LS – right ventricular global  
8 longitudinal strain (lateral wall and septum); RVEF – right ventricular ejection fraction; RV wall  
9 average LS - lateral, anterior and inferior wall LS all feasible.

10 Figure 4. Bland Altman plots demonstrating agreement between right ventricular functional  
11 parameters derived by TTE and CMR. Left panel – right ventricular ejection fraction (RVEF);  
12 centre panel – RV lateral (free) wall longitudinal strain; right panel – RV global LS (lateral wall  
13 and septum).

14 Figure 5. Receiver operating characteristic curves displaying the ability of right ventricular  
15 echocardiographic functional parameters to identify diminished CMR-derived right ventricular  
16 ejection fraction (RVEF <45%). AUC – area under the curve. \*p <0.05 for RV global LS vs RV  
17 lateral wall LS and RV global LS vs TAPSE.

18 Figure 6. Suggested approach to right ventricular functional assessment by transthoracic  
19 echocardiography in ACHD patients.

20

21

1 **Tables****Table 1. Baseline characteristics and transthoracic echocardiography**

	ACHD patients (n = 100)
<i>Demographics</i>	
Age, years	50 ± 5
Sex (male), n	53
Body mass index, kg/m <sup>2</sup>	26.5 ± 4.6
Systolic blood pressure, mmHg	132 ± 16
Diastolic blood pressure, mmHg	82 ± 12
<i>Electrocardiogram</i>	
Sinus rhythm, n	94
Atrial rhythm, n	6
QRS duration, ms	109 [95, 126]
<i>Congenital group and cardiothoracic intervention</i>	
Corrected atrial septal defect, n	48
Repaired Tetralogy of Fallot, n	32
Pulmonary stenosis, n	20
Age at definitive surgical correction, years	6 [3, 8]
Surgical re-intervention, n	25
<i>Transthoracic echocardiography</i>	
Right ventricular basal dimension, mm (n = 90)	44 [40, 49]
Right ventricular mid dimension, mm (n = 79)	33 [30, 38]
Right ventricular longitudinal dimension, mm (n = 86)	86 ± 10

Right ventricular outflow tract 1 dimension, mm (n = 65)	38 ± 5
3D RV end diastolic volume index, ml/m <sup>2</sup>	74 [61, 88]
3D RV end systolic volume index, ml/m <sup>2</sup>	38 [33, 50]
Right atrial area, cm <sup>2</sup> (n = 86)	19 [16, 22]
≥ Moderate pulmonary regurgitation, n	11
≥ Moderate pulmonary stenosis, n	8
≥ Moderate tricuspid regurgitation, n	5
Tricuspid regurgitation maximum velocity, m/s (n = 83)	2.4 [2.2, 2.6]
Systolic pulmonary artery pressure, mmHg (n =83)	28 [24, 34]
Pulmonary valve peak gradient, mmHg (n = 99)	9 [5, 18]
Left heart function, n (%):	
Significantly impaired systolic function (LVEF ≤45%)	1
Grade II-III diastolic function	5
≥ Moderate left sided valvular disease	0

---

Data is presented as mean ± standard deviation, as median [25<sup>th</sup>, 75<sup>th</sup> percentile]

or number. RV – right ventricle; LVEF – left ventricular ejection fraction.

1  
2  
3  
4

**Table 2. Associations of echocardiographic right ventricular functional parameters with cardiovascular magnetic resonance derived right ventricular ejection fraction**

	No. comparisons	TTE values	CMR values	r	p-value
<i>RV two-dimensional conventional echo</i>					
TAPSE, mm	98	17 ± 3		0.16	0.06
RV S', cm/s	93	10 ± 2		0.23	<b>0.015</b>
Fractional area change, %	67	38 ± 7		0.48	<b>&lt;0.001</b>
<i>RV three dimensional echo</i>					
3D RV ejection fraction, %	48	46 ± 6	51 ± 6	0.40	<b>0.005</b>
<i>RV multi-plane echo longitudinal strain (LS), %</i>					
Global LS (lateral wall and septum)	55	-18 ± 5	-24 ± 4	-0.62	<b>&lt;0.001</b>
Lateral (free) wall LS	56	-22 ± 5	-29 ± 5	-0.45	<b>&lt;0.001</b>
Anterior wall LS	35	-20 ± 4		-0.41	<b>0.007</b>
Inferior wall LS	47	-22 ± 4		-0.22	0.07
Inferior coronal view wall LS	30	-19 ± 4*		-0.08	0.34
RV wall average LS	34	-21 ± 4		-0.49	<b>0.002</b>

Data is presented as mean ± standard deviation with r- and p-values reflecting correlation of TTE values with CMR-RVEF. RV wall average LS calculated when lateral, anterior and inferior walls all feasible to measure. \*p <0.01 vs RV lateral wall LS. RV – right ventricle; TAPSE – tricuspid annular plane systolic excursion; RV S' – tissue Doppler imaging derived tricuspid annular peak systolic velocity.

**Table 3. Right ventricular functional analysis by cardiovascular magnetic resonance.**

	All ACHD patients	Patients with feasible TTE measurements*	p-value
Volumetric (n = 100)			
RV end diastolic volume index, ml/m <sup>2</sup>	98 [82, 117]	100 [86, 119]	0.49
RV end systolic volume index, ml/m <sup>2</sup>	47 [39, 61]	49 [40, 60]	0.84
RV ejection fraction, %	50 ± 8	51 ± 6	0.49
Feature-tracking (n = 98)			
RV free wall longitudinal strain, %	-30 ± 5	-29 ± 5	0.61
RV global longitudinal strain, %	-25 ± 4	-24 ± 4	0.73

Data is presented as mean ± standard deviation or as median [25<sup>th</sup>, 75<sup>th</sup> percentile]. \* Volumetric data n = 48;

RV free wall longitudinal strain n = 56; RV global longitudinal strain n = 55. RV – right ventricle.

**Table 4. Receiver operating characteristics and optimal cut-off values of echocardiographic parameters to identify reduced right ventricular ejection fraction (<45%) by cardiovascular magnetic resonance.**

	AUC (95% CI)	p-value	Cut-off	Sens.	Spec.	Youden-J Index
TAPSE (n = 98)	0.60 (0.46-0.74)*	0.15	18	68	53	0.21
RV S' (n = 93)	0.63 (0.49-0.77)	0.07	11	76	36	0.12
Fractional area change (n = 67)	0.68 (0.52-0.83)*	<b>0.045</b>	35	57	76	0.33
3D right ventricular ejection fraction (n = 48)	0.71 (0.49-0.93)	0.10	44	83	62	0.45
Global LS (lateral wall and septum, n = 55)	0.84 (0.72-0.96)	<b>&lt;0.001</b>	-19	100	57	0.57
Lateral wall LS (n = 56)	0.76 (0.60-0.92)*	<b>0.009</b>	-21	73	67	0.40
Anterior wall LS (n = 35)	0.81 (0.63-0.98)	<b>0.010</b>	-19	88	78	0.65
Inferior wall LS (n = 47)	0.67 (0.48-0.86)*	0.10	-20	70	57	0.27
Inferior coronal view wall LS (n = 30)	0.60 (0.37-0.83)	0.40	-19	67	71	0.38
RV wall average LS (n = 34)	0.82 (0.66-0.98)	<b>0.007</b>	-21	88	65	0.53

Cut-off value used in receiver operating characteristics analysis defined as CMR-derived RVEF of 45%. RV wall average LS calculated when lateral, anterior and inferior walls all feasible to measure.\* p <0.05 for AUC vs Global LS. TAPSE – tricuspid annular plane systolic excursion; RV S' – tissue Doppler imaging derived tricuspid annular peak systolic velocity; LS – longitudinal strain; AUC – area under the curve; CI – confidence interval.



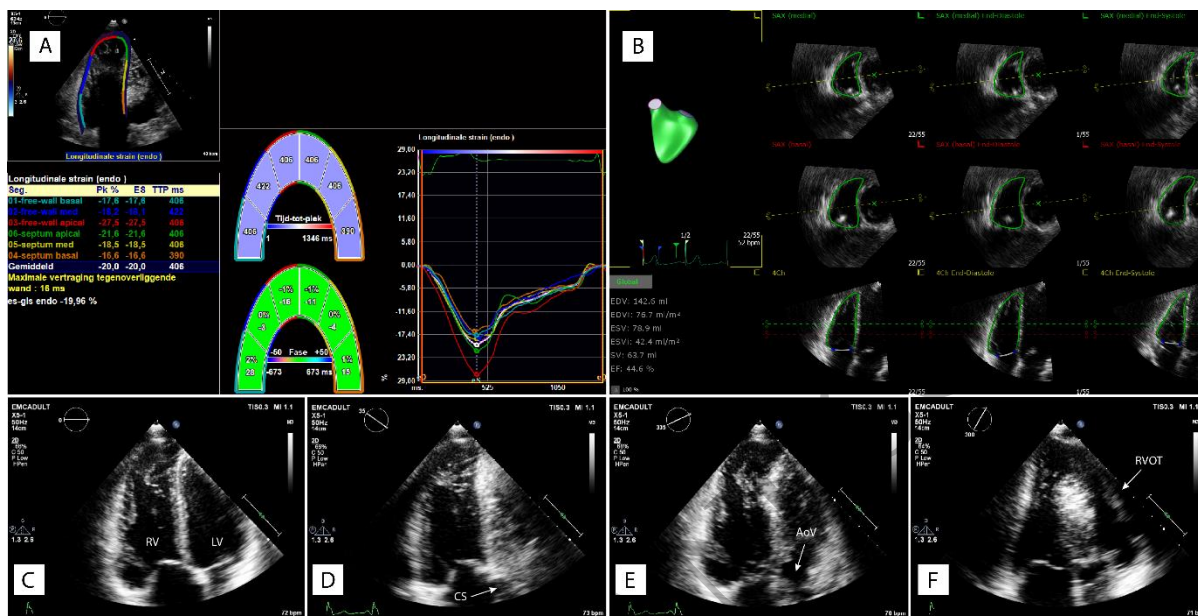


Figure 1  
159x81 mm (x DPI)

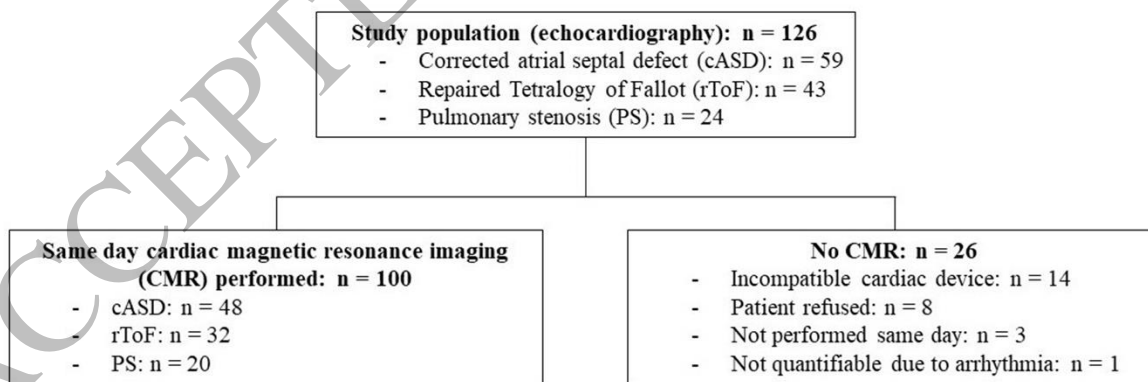


Figure 2  
159x55 mm (x DPI)

1  
2  
3  
4  
5  
6  
7  
8  
9  
10

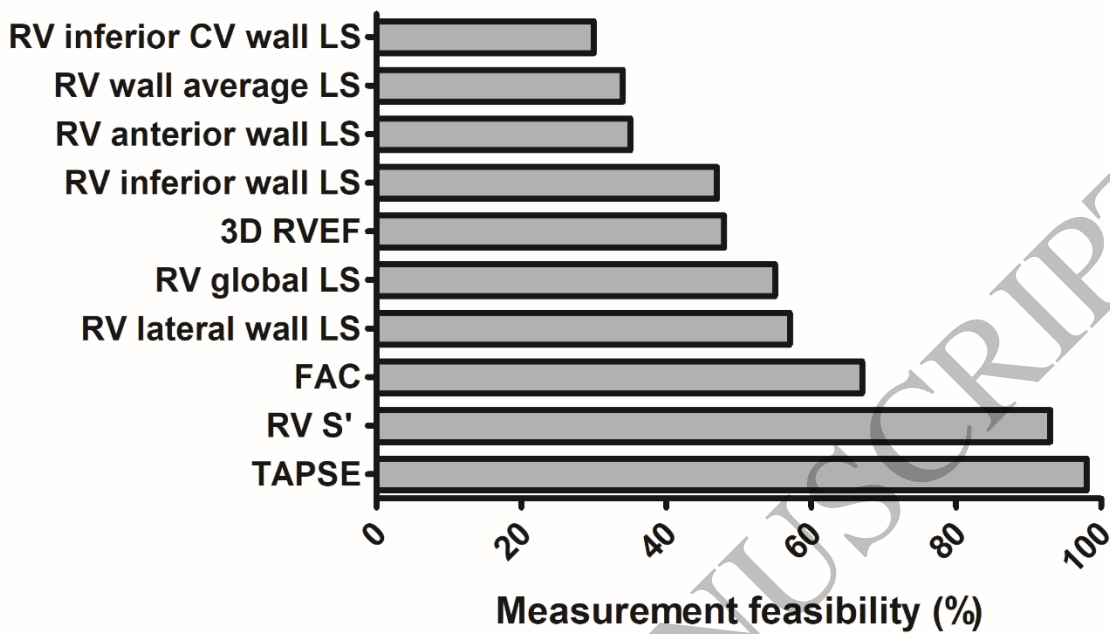


Figure 3  
159x92 mm (x DPI)

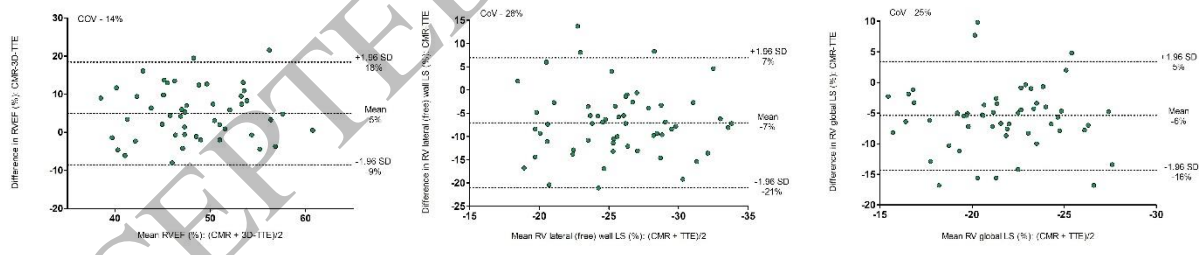


Figure 4  
159x35 mm (x DPI)

1  
2  
3  
4  
5  
6  
7  
8  
9  
10

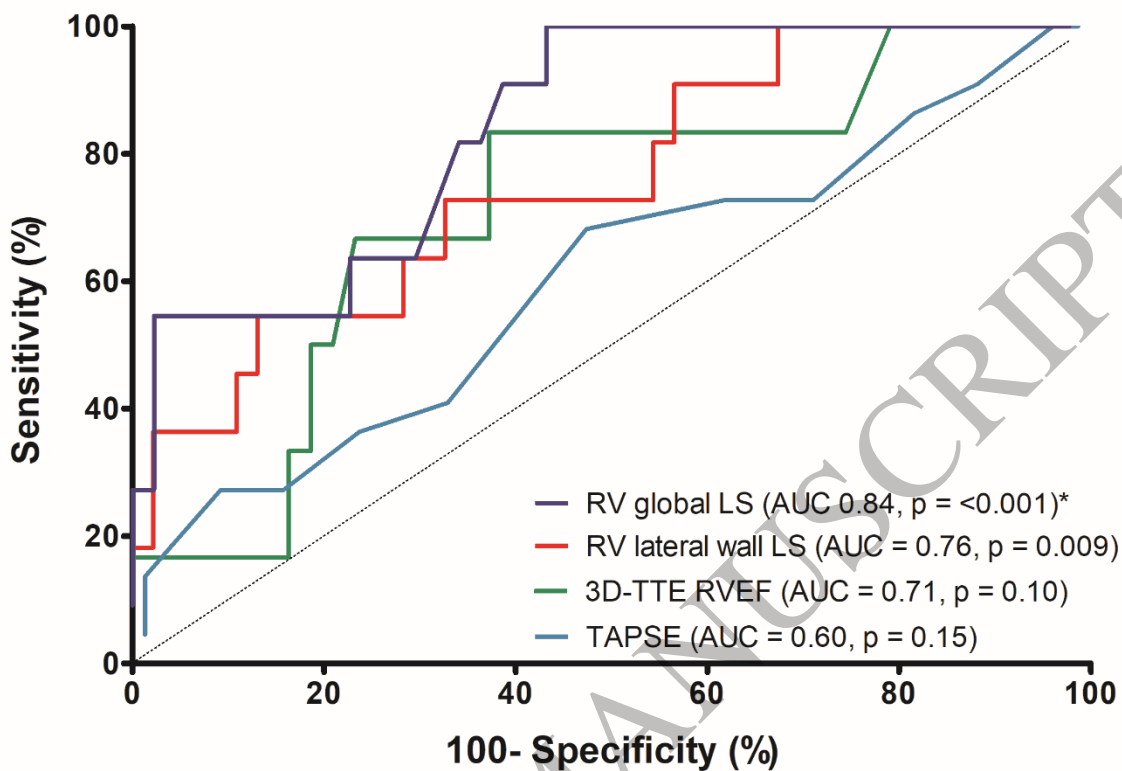


Figure 5  
159x108 mm ( x DPI)

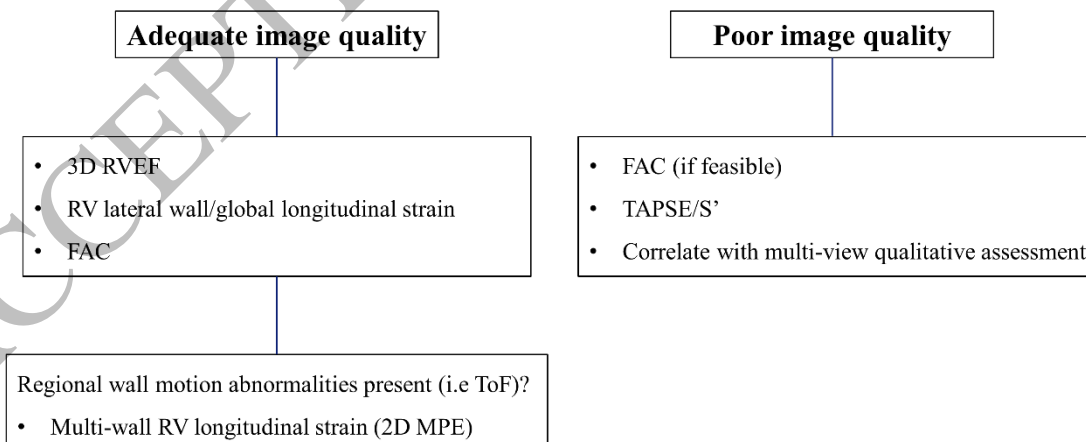


Figure 6  
159x64 mm ( x DPI)

1  
2  
3  
4  
5  
6  
7  
8  
9

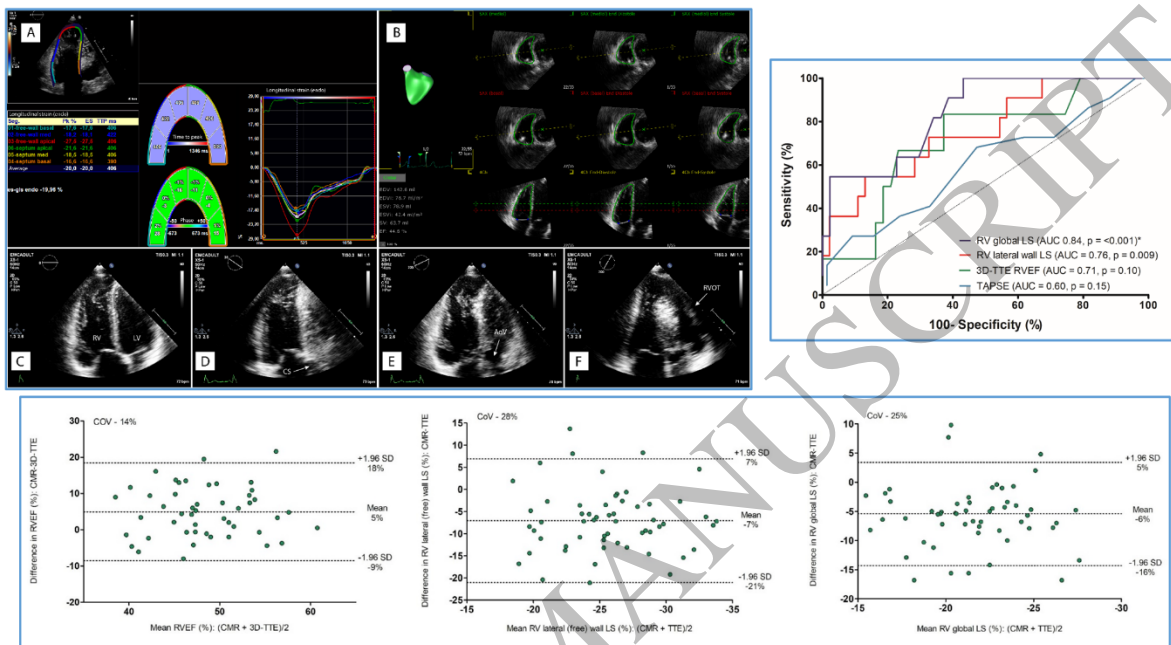
Study evaluating association of advanced TTE RV functional parameters with CMR-derived RV function in 100 ACHD patients

- Upper left panel: A – RV longitudinal strain (LS); B – RV ejection fraction (3D-RVEF); C-F – 2D multi-plane echo of four RV free wall regions.

• 3D-RVEF, RV LS and fractional area change were moderately correlated with CMR-RVEF.

- RV global LS correlated strongest ( $r -0.62$ ) and best identified reduced CMR-RVEF <45% (upper right panel).

• Significant differences exist between indices measurable by both modalities (Lower panel L-R - RVEF, RV free wall LS, RV global LS).



Graphical Abstract  
159x111 mm ( x DPI)

1  
2  
3